doi.org/10.26434/chemrxiv.12033303.v1

Bioreducible Pro-drug Inhibitors of Enolase

Victoria Yan, Kristine Yang, Elliot Ballato, Kenisha Arthur, Dimitra Georgiou, Florian Muller

Submitted date: 26/03/2020 • Posted date: 26/03/2020

Citation information: Yan, Victoria; Yang, Kristine; Ballato, Elliot; Arthur, Kenisha; Georgiou, Dimitra; Muller, Florian (2020): Bioreducible Pro-drug Inhibitors of Enolase. ChemRxiv. Preprint. https://doi.org/10.26434/chemrxiv.12033303.v1

Glycolysis inhibition remains aspirational in cancer therapy. We recently described a promising phosphonate inhibitor of Enolase for cancers harboring deletions in ENO1. Here, we describe the application of nitroheterocycle pro-drugs capitalizing on tumor hypoxia. These bioreducible pro-drugs exhibit up to 14-fold greater potency under hypoxic conditions compared to normoxia and exhibit robust stability in biological fluids. Our work provides strong proof-of-concept for using bioreduction as a pro-drug delivery strategy in the context of Enolase inhibition.

Bioreducible Pro-drug Inhibitors of Enolase

Victoria C. Yan, Kristine L. Yang, Elliot S. Ballato, Kenisha Arthur, Dimitra K. Georgiou, and Florian L. Muller*

Department of Cancer Systems Imaging, University of Texas MD Anderson Cancer Center, Houston, Texas, 77054

KEYWORDS: pro-drug, hypoxia, glycolysis inhibitor, targeted therapy

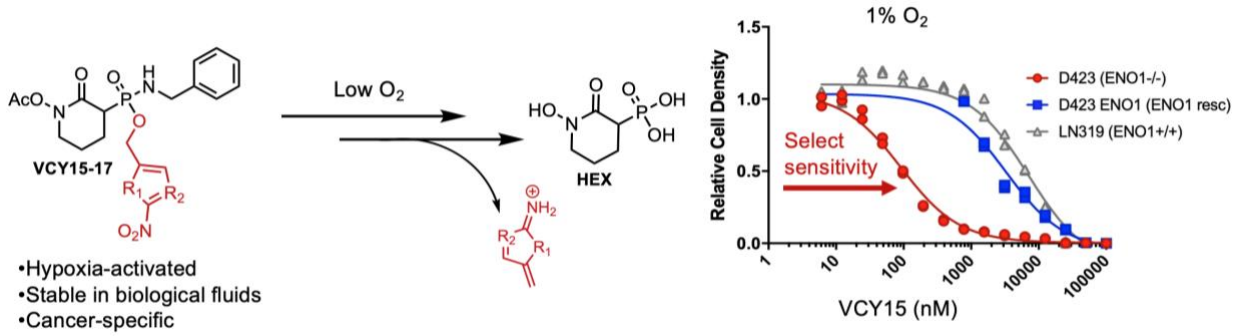

ABSTRACT: Glycolysis inhibition remains aspirational in cancer therapy. We recently described a promising phosphonate inhibitor of Enolase for cancers harboring deletions in ENO1. Here, we describe the application of nitroheterocycle pro-drugs capitalizing on tumor hypoxia. These bioreducible pro-drugs exhibit up to 14-fold greater potency under hypoxic conditions compared to normoxia and exhibit robust stability in biological fluids. Our work provides strong proof-of-concept for using bioreduction as a pro-drug delivery strategy in the context of Enolase inhibition.

Glioblastoma multiforme (GBM) is a highly aggressive form of brain cancer, with few patients surviving beyond 2.5 years[1]. Targeting vulnerabilities in cellular metabolism represents a promising, emergent strategy in precision oncology. We previously described one such vulnerability in glycolysis, in which the gene encoding for the enzyme Enolase, *ENO1*, undergoes homozygous deletion in a subset of GBMs[2–4]. Cancers harboring the homozygous deletion *ENO1* remain metabolically active and viable through redundant action of its paralogue, ENO2. Inhibition of ENO2 in *ENO1*-deleted cancers results in cancer-specific killing, leaving non-malignant tissue unperturbed[2,5,6].

A central challenge to developing a therapeutically relevant Enolase inhibitor concerns the highly polar nature of glycolysis metabolites, resulting in highly polar inhibitor structures. To this end, we recently reported the design and synthesis of a phosphonate-containing ENO2-inhibitor, termed "HEX." Because phosphonates are negatively charged at physiological pH, a pivaloyloxymethyl (POM)-prodrug derivative, "POMHEX," was initially synthesized to improve cell peremeaebility[7]. While POMHEX shows exceptional, preferential potency against ENO1-deleted cells in vitro and can eradicate ENO1-deleted tumors in preclinical murine models, it suffers from poor pharmacokinetics. Rapid, extracellular cleavage of the first POM group by high concentrations of carboxylesterases exposes the negatively charged phosphonate monoester—reintroducing cell and blood-brain-barrier (BBB) permeability issues.

The most optimal prodrug delivery system avoids premature extracellular cleavage and enables selective release of the active agent within the tumor. A common feature of many tumors, especially GBM, is the presence of highly hypoxic areas[8], in which median oxygen levels may be as low as ~2%, as compared to ~7% in normal tissue[9]. At present, hypoxia is visualized clinically using agents such as ^{18}F-AZA and histologically via pimonidazole[10,11]. Common to both probes is the inclusion of a nitroimidazole moiety, which can be reduced under hypoxic condition through nitroreductases (NADH dehydrogenases), to reveal the active agent[12]. Here, we are the first to demonstrate the feasibility of using bioreducible prodrugs as a stable, tunable method for the targeted delivery of a phosphonate glycolysis inhibitor.

The polyprotic nature of phosphates warrants the attachment of two prodrug protecting groups for efficient cell permeation. While nitroreductases can facilitate the removal of the first prodrug moiety, hydrolysis of the second pro-drug is limited to enzymes that can tolerate the presence of an anionic substrate. We recognized phosphoramidases[13] as a class of enzymes fulfilling this requirement and thus sought to synthesize mixed phosphoramidate esters (**Figure 1**).

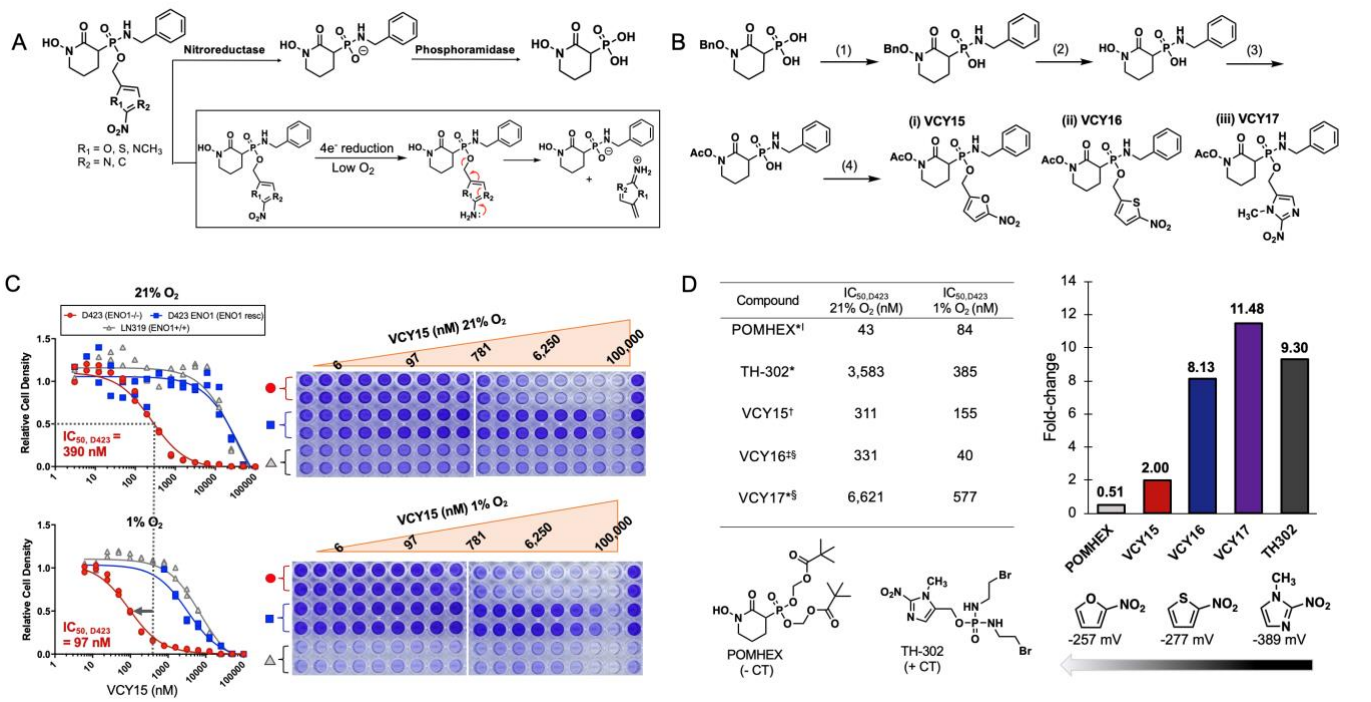

Figure 1. Nitroaromatic benzylamine pro-drugs exhibit greater potency under hypoxic conditions. (**A**) Mechanism of bioactivation under low O_2 conditions. **(B)** Synthesis of nitroaromatic benzylamine pro-drugs. Reaction conditions: (1) EDC, $BnNH_2$ in acetone/H_2O, 15 h, (2) H_2, Pd/C in THF/MeOH, 3 h, (3) Ac_2O in MeCN, 3h, (4) a.) 2-(bromomethyl)-5-nitrofuran in MeCN, 15 h, b.) 2-(bromomethyl)-5-nitrothiophene in MeCN, 15 h, c.) (1-methyl-2-nitro-1*H*-imidazol-5-yl)methanol, PPh_3/DIAD, $CHCl_3$. For detailed synthetic procedures, see Supporting Information. (**C**) Representative inhibitory curves and plates for VCY15 at 21% O_2 (top) and 1% O2 (bottom); in both conditions, VCY15 is selective for D423 (*ENO1*-deleted) cells. (**D**) Average potency comparisons for various nitroaromatic benzylamine pro-drugs at 21% and 1% O_2. *n=1, †n=5, ‡n=2, §Compounds were determined pure by ^{31}P NMR but contained contaminants visible in ^{1}H and ^{13}C spectra. ǀTested for 4 days.

Benzyl-protected HEX (BnHEX), was prepared according to previously published procedures[7]. First, BnHEX was coupled with benzylamine using 1-ethyl-3-(3-dimethylaminopropyl)carbodiimide to generate the intermediate phosphoramidate (Scheme 2). We then performed reductive hydrogenation to remove the benzyl ether and then re-protected the hydroxamate with an acetyl group. Though circuitous, we found these deprotection-reprotection steps to be necessary for further reaction with the nitroheterocycles. Due to the nucleophilic nature of the hydroxamate, direct reaction with the nitroheterocycles was not possible without addition to the hydroxamate.

To examine the relationship between standard reduction potential and sensitivity to hypoxia, we attached three nitroheterocycle derivatives: a nitrofuran (Scheme 2a, VCY15), nitrothiophene (Scheme 2b, VCY16), or a nitroimidazole (Scheme2c, VCY17). Both the nitrofuran and the nitrothiophene prodrugs were generated by simple S_n2 reaction with the phosphoramidate intermediate to generate VCY15 and VCY16, respectively. The nitroimidazole, VCY17, was attached using a Mitsunobu coupling with the phosphoramidate.

Previous studies have shown that nitroreductases facilitate the removal of nitroheterocycles under hypoxic conditions through a 4-electron reduction mechanism[12]. It thus followed that the ease of reduction would depend on the standard reduction potentials of the nitroheterocycles. Upon examining of the redox potentials for nitrofuran, nitrothiophene, and nitroimidazole, we hypothesized that hypoxia-mediated bioactivation towards the active compound would correlate with the standard reduction potentials of these nitroheterocycles. Standard reduction potentials have been reported as follows: nitrofurans, -257 mV[14]; nitrothiophenes, -277 mV[15] ;and nitroimidazoles, -398 mV[14]. Accordingly, VCY15 (**Figure 1b, i**) would be least sensitive, while VCY16 (**Figure 1b, ii**) and VCY17 (**Figure 1b, iii**) would show intermediate and dramatic sensitivities, respectively. To test this, we performed in vitro cell culture experiments under both normoxia (21% O_2) and hypoxia (1% O_2). We note that while the physiological oxygen concentration ("physioxia") is about 7% O_2[16], we saw no significant difference in cytotoxicity measurements between 21% O_2 and 7% O_2 (**Supporting Information Figure S8**). All three compounds were tested against three cell lines: D423 (*ENO1*-deleted), D423 ENO1 (ENO1 overexpressing), and LN319 (wild-type control). Cells were incubated with VCY15, VCY16, VCY17, and at 21% O_2 or 1% O_2. At the same time, we also tested a non-bioreducible pro-drug, POMHEX (negative control) and a bioreducible pro-drug alkylating agent (TH-302, positive control. After 5 days, cells were then fixed, stained with crystal violet, and quantified spectroscopically. All three nitroheterocycle pro-drugs showed selectivity for D423 cells, indicating selective inhibition of Enolase through release of the active agent, HEX. Importantly, VCY15-17 showed markedly improved potency under hypoxic conditions compared to the POMHEX, which contains no bioreducible moieties (**Figure 1d**). Amongst the three pro-drugs, VCY15 exhibited the greatest overall potency, with an IC_{50} of ~ 311 nM at 21% O_2 and of ~155 nM at 1% O_2 (**Figure 1d**). For comparison, VCY16 and VCY17 exhibited IC_{50}s of 331 nM and 6622 nM at 21% O_2 and 41 nM and 557 nM, respectively (**Figure 1d**). Concurrent with our

predictions, the potency changes from normoxia to hypoxia correlated with the standard redox potentials of each

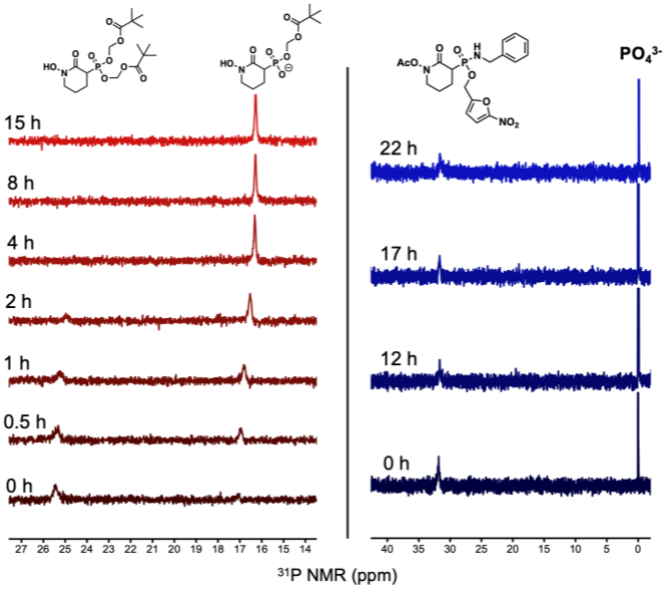

Figure 2. Nitroaromatic benzylamine pro-drugs exhibit robust stability in human plasma. ^{31}P NMR scans (121 MHz) of esterase-labile pro-drug, POMHEX (left, red) and VCY15 (right, blue) were taken in 80% human plasma with 20% D_2O for signal lock; ns = 1000. Where POMHEX degrades to its hemi-ester form after 4 hours, VCY15 remains stable for over 22 hours.

nitroheterocycle. At 1% O2, VCY15 (nitrofuran) exhibited a 2-fold increase in potency, VCY16 (nitrothiophene) exhibited an 8-fold increase in potency, and VCY17 (nitroimidazole) exhibited a 12-fold increase in potency (**Figure 1d**). Combined, the above results suggest a correlation between cytotoxicity and pro-drug sensitivity to O_2; this corresponds with studies on various nitroaromatic derivatives conjugated to alkylating agents[17] or radiosensitizers[18]. While VCY17 exhibits the greatest fold-change in potency, it is seemingly the least potent pro-drug according to absolute IC_{50} values at both 21% and 1% O_2. This may be explained by the necessity of extremely low oxygen concentrations for cleavage of the first pro-drug moiety. By extension, the lower IC_{50} values of VCY15 may be attributed to the higher reduction potential of the nitrofuran, which does not require severely low levels of oxygen for nitroreductase-mediated cleavage.

Finally, we sought to examine the stability of these nitroheterocycle pro-drugs in human plasma. We reasoned that VCY15-17 should experience little to no degradation, as nitroreductases are found exclusively within the cell and intracellular phosphoramidases require the presence of a negative charge for hydrolytic activity. To examine stability, we assayed VCY15-17 at various timepoints in human plasma using ^{31}P NMR (**Figure 2**). In sharp contrast to POMHEX, which begins to hydrolyze to its monoester form in less than 30 minutes (**Figure 2, left**), all nitroheterocycle prodrugs were stable for over 22 hours (**Figure 2, right**), as indicated by a constant peak at ~32 ppm.

In sum, we have prepared a set of nitroheterocycle prodrugs that confer vastly improved specificity and stability towards cancer cells. Our data show that this delivery mechanism is specific to tumors, in which extended hypoxia is a unique characteristic. For the purposes of targeting cancer metabolism, we have herein demonstrated the unprecedented, targeted delivery of a negatively charged glycolysis inhibitor using bioreduction. That our work evidences the viability of using bioreducible prodrugs to vastly improve target specificity may also shift general attitudes on phosphonates from a liability to a potential asset, especially in the age of personalized therapy.

ASSOCIATED CONTENT

Supporting Information

The Supporting Information is available free of charge on the ACS Publications website.

Compound characterization, cell culture experiments (PDF)

AUTHOR INFORMATION

Corresponding Author

* F.L.M.: aettius@aol.com

Author Contributions

V.C.Y., K.L.Y., and E.S.B. performed syntheses and purifications. V.C.Y. and E.S.B. characterized compounds. K.A. and D.K.G., performed cell culture experiments. V.C.Y. and F.L.M. performed data analysis. V.C.Y. wrote the manuscript. F.L.M. oversaw overall project design

ACKNOWLEDGMENTS

We thank Kumar Kalhurachchi for NMR assistance. We thank Theresa Tran, Anton Poral, and Mykia Washington for assistance with cell culture experiments. Funding from the American Cancer Society (RSG-15-145-01-CDD) and the National Comprehensive Cancer Network (YIA170032) is gratefully acknowledged.

REFERENCES

(1) Schwartzbaum, J. A.; Fisher, J. L.; Aldape, K. D.; Wrensch, M. Epidemiology and Molecular Pathology of Glioma. *Nat. Clin. Pract. Neurol.* **2006**, *2* (9), 494–503.

(2) Muller, F. L.; Colla, S.; Aquilanti, E.; Manzo, V. E.; Genovese, G.; Lee, J.; Eisenson, D.; Narurkar, R.; Deng, P.; Nezi, L.; et al. Passenger Deletions Generate Therapeutic Vulnerabilities in Cancer. *Nature* **2012**, *488*, 337–343.

(3) Ichimura, K.; Vogazianou, A. P.; Liu, L.; Pearson, D. M.; Bäcklund, L. M.; Plant, K.; Baird, K.; Langford, C. F.; Gregory, S. G.; Collins, V. P. 1p36 Is a Preferential Target of Chromosome 1 Deletions in Astrocytic Tumours and Homozygously Deleted in a Subset of Glioblastomas. *Oncogene* **2008**, *27* (14), 2097–2108.

(4) Duncan, C. G.; Killela, P. J.; Payne, C. A.; Lampson, B.; Chen, W. C.; Liu, J.; Solomon, D.; Waldman, T.; Towers, A. J.; Gregory, S. G.; et al. Integrated Genomic Analyses Identify ERRFI1 and TACC3 as Glioblastoma-Targeted Genes. *Oncotarget* **2010**, *1* (4), 265.

(5) Leonard, P. G.; Satani, N.; Maxwell, D.; Lin, Y.-H.; Hammoudi, N.; Peng, Z.; Pisaneschi, F.; Link, T. M.; Lee, G. R.; Sun, D.; et al. SF2312 Is a Natural Phosphonate Inhibitor of Enolase. *Nat. Chem. Biol.* **2016**, *12* (12), 1053–1058.

(6) Muller, F. L.; Aquilanti, E. A.; DePinho, R. A. Collateral Lethality: A New Therapeutic Strategy in Oncology. *Trends in Cancer* **2015**, *1* (3), 161–173.

(7) Lin, Y.-H.; Satani, N.; Hammoudi, N.; Ackroyd, J. J.; Khadka, S.; Yan, V. C.; Georgiou, D. K.; Sun, Y.; Zielinski, R.; Tran, T.; et al. Eradication of ENO1-Deleted Glioblastoma through Collateral Lethality. *bioRxiv* **2018**, 331538.

(8) Brown, J. M. Tumor Hypoxia in Cancer Therapy. *Methods*

Enzymol. **2007**, *435*, 295–321.

(9) Vaupel, P.; Höckel, M.; Mayer, A. Detection and Characterization of Tumor Hypoxia Using PO2 Histography. *Antioxid. Redox Signal.* **2007**, *9* (8), 1221–1236.

(10) Beck, R.; Röper, B.; Carlsen, J. M.; Huisman, M. C.; Lebschi, J. A.; Andratschke, N.; Picchio, M.; Souvatzoglou, M.; Machulla, H.-J.; Piert, M. Pretreatment 18F-FAZA PET Predicts Success of Hypoxia-Directed Radiochemotherapy Using Tirapazamine. *J. Nucl. Med.* **2007**, *48* (6), 973–980.

(11) Varia, M. A.; Calkins-Adams, D. P.; Rinker, L. H.; Kennedy, A. S.; Novotny, D. B.; Fowler, W. C.; Raleigh, J. A. Pimonidazole: A Novel Hypoxia Marker for Complementary Study of Tumor Hypoxia and Cell Proliferation in Cervical Carcinoma. *Gynecol. Oncol.* **1998**, *71* (2), 270–277.

(12) Wilson, W. R.; Hay, M. P. Targeting Hypoxia in Cancer Therapy. *Nat. Rev. Cancer* **2011**, *11* (6), 393–410.

(13) McGuigan, C.; Madela, K.; Aljarah, M.; Bourdin, C.; Arrica, M.; Barrett, E.; Jones, S.; Kolykhalov, A.; Bleiman, B.; Bryant, K. D.; et al. Phosphorodiamidates as a Promising New Phosphate Prodrug Motif for Antiviral Drug Discovery: Application to Anti-HCV Agents. *J. Med. Chem.* **2011**, *54* (24), 8632–8645.

(14) Wardman, P.; Clarke, E. D. Oxygen Inhibition of Nitroreductase: Electron Transfer from Nitro Radical-Anions to Oxygen. *Biochem. Biophys. Res. Commun.* **1976**, *69* (4), 942–949.

(15) Tercel, M.; Lee, A. E.; Hogg, A.; Anderson, R. F.; Lee, H. H.; Siim, B. G.; Denny, W. A.; Wilson, W. R. Hypoxia-Selective Antitumor Agents. 16. Nitroarylmethyl Quaternary Salts as Bioreductive Prodrugs of the Alkylating Agent Mechlorethamine. *J. Med. Chem.* **2001**, *44* (21), 3511–3522.

(16) McKeown, S. R. Defining Normoxia, Physoxia and Hypoxia in Tumours-Implications for Treatment Response. *Br. J. Radiol.* **2014**, *87* (1035), 20130676.

(17) Naylor, M. A.; Stephens, M. A.; Cole, S.; Threadgill, M. D.; Stratford, I. J.; O'neill, P.; Fielden, E. M.; Adams, G. E. *Synthesis and Evaluation of Novel Electrophilic Nitrofuran Carboxamides and Carboxylates as Radiosensitizers and Bioreductively Activated Cytotoxins*; 1990.

(18) Adams, G. E.; Clarke, E. D.; Flockhart, I. R.; Jacobs, R. S.; Sehmi, D. S.; Stratford, I. J.; Wardman, P.; Watts, M. E.; Parrick, J.; Wallace, R. G.; et al. Structure-Activity Relationships in the Development of Hypoxic Cell Radiosensitizers. *Int. J. Radiat. Biol. Relat. Stud. Physics, Chem. Med.* **1979**, *35* (2), 133–150.

SYNOPSIS TOC (Word Style "SN_Synopsis_TOC"). If you are submitting your paper to a journal that requires a synopsis graphic and/or synopsis paragraph, see the Instructions for Authors on the journal's homepage for a description of what needs to be provided and for the size requirements of the artwork.

To format double-column figures, schemes, charts, and tables, use the following instructions:

Place the insertion point where you want to change the number of columns
From the **Insert** menu, choose **Break**
Under **Sections**, choose **Continuous**
Make sure the insertion point is in the new section. From the **Format** menu, choose **Columns**
In the **Number of Columns** box, type **1**
Choose the **OK** button

Now your page is set up so that figures, schemes, charts, and tables can span two columns. These must appear at the top of the page. Be sure to add another section break after the table and change it back to two columns with a spacing of 0.33 in.

Table 1. Example of a Double-Column Table

Column 1	Column 2	Column 3	Column 4	Column 5	Column 6	Column 7	Column 8

Authors are required to submit a graphic entry for the Table of Contents (TOC) that, in conjunction with the manuscript title, should give the reader a representative idea of one of the following: A key structure, reaction, equation, concept, or theorem, etc., that is discussed in the manuscript. Consult the journal's Instructions for Authors for TOC graphic specifications.

Insert Table of Contents artwork here

Supporting Online Material for

Bioreducible Pro-drug Inhibitors of Enolase Targeting *ENO1*-Deleted Glioblastoma

Victoria C. Yan, Kristine L. Yang, Elliot S. Ballato, Kenisha Arthur, Dimitra K. Georgiou, and Florian L. Muller*

*aettius@aol.com

Department of Cancer Systems Imaging, University of Texas MD Anderson Cancer Center

Houston, Texas, 77054, United States

Table of Contents

1. General information ***S2***

2. Synthetic procedures ***S3***

3. Cell culture experiments ***S5***

4. References ***S8***

1. General Information

General synthetic procedures. All solvents and reagents were purchased from Sigma-Aldrich at the highest commercially available purity and were used without further purification. ^{1}H, ^{13}C, and ^{31}P, NMR were recorded on a Bruker Avance 500 MHz or 300 MHz spectrometer, as indicated. BnHEX was initially synthesized according to previously published procedures[1]; subsequent syntheses were contracted to WuXi AppTec, Shanghai, China. Final compounds were purified via HPLC (Phenomenex Luna-C18. 0-3 min 10% Buffer B, 21-24 min 100% Buffer B, 27-30 min, 10% Buffer B; Buffer A= H_2O + 0.1% TFA, Buffer B= MeCN + 0.01% TFA). See Figure 1b for a representative synthesis scheme.

General cell culture procedure. Cell culture experiments were conducted using the D423-MG cell line. 1p36 homozygous deletion in D423 includes the genes from *CAMTA1 to SLC25A33*; this includes *ENO1*. Isogenic *ENO1* ectopically rescued lines were described previously (pCMV ENO1 5X)[2]. An *ENO1*-intact cell line (LN319) was used as a control for sensitivity to Enolase inhibitors. Cells were routinely cultured in Dulbecco's modified Eagle's medium supplemented with 10% fetal bovine serum.

Abbreviations used: TFA—trifluoroacetic acid, THF—tetrahydrofuran, MeOH—methanol, MeCN—acetonitrile, EDC—1-Ethyl-3-(3dimethylaminopropyl)carbodiimide, DIAD—diisopropyl azodicarboxylate

2. Synthetic procedures

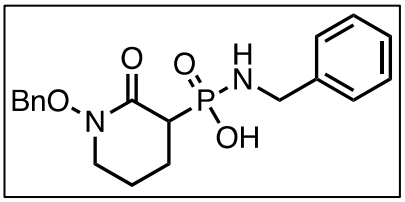

N-benzyl-P-(1-(benzyloxy)-2-oxopiperidin-3-yl)phosphonamidic acid (1) (1-(benzyloxy)-2-oxopiperidin-3-yl)phosphonic acid. (1-(benzyloxy)-2-oxopiperidin-3-yl)phosphonic acid (125.0 mg, 438 mmol, BnHEX**)** was dissolved in 150 mL acetone. To this solution, benzylamine (2.21g, 2.25 mL, 21mmol, **2**) and EDC (600 mg, 5.6 mmol, dissolved in a mixture of 2.5 mL acetone and 7.5 mL $CHCl_3$)were added over the course of 4 h. H_2O was added periodically, up to a total volume of 14 mL, to keep reagents in solution. The reaction was continuously stirred for an additional 20 h until completion. Then, the reaction was extracted with 1 equivalent of ddH_2O and then 1 M HCl. Next, the reaction was neutralized with .01 volumes of saturated $NaHCO_3$. The organic layer was kept, dried over $NaSO_4$, and rotavapped down to 10 mL. This was then diluted with three volumes of hexanes, and this mixture was extracted with one volume of ddH_2O. The aqueous layer was kept and lyophilized for 2 days to an amber oil. Analysis by ESI+ (Expected $[M+H]^+$=375.38. Observed $[M+H]^+$=375). **^{1}H NMR** (500 MHz, D_2O) δ 7.32-7.53 (m, 5 H), 4.91-4.96 (m, 2H), 4.02-4.11 (m, 2H)), 3.46-3.57 (m, 2H), 2.80-2.87 (dt, J=21.52 Hz, J=21.70 Hz, 1H), 2.07-2.13 (m, 1H), 1.92-1.98 (m, 2H), 1.72-1.79 (m, 1H). **^{13}C NMR** (125.7 MHz, D_2O) δ 167.97 (d, J=4.72 Hz, 1C), 141.25 (d, J=7.36 Hz, 1C), 134.52 (s, 1C), 129.92 (s, 2C), 129.15 (s, 1C), 128.73 (s, 2C), 128.60 (s, 2C), 127.59 (s, 1C), 127.00 (s, 1C), 75.54 (s, 1C), 50.11 (s, 1C), 45.28 (s, 1C), 43.64 (d, J=111.12 Hz, 1C), 22.33 (d, J=3.65 Hz, 1C), 21.65 (d, J=7.23 Hz, 1C). **^{31}P NMR** (202 MHz, D_2O) δ 20.91.

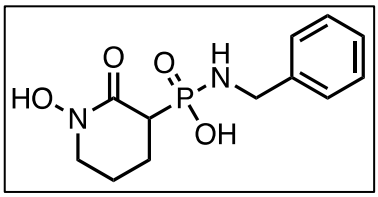

(N-benzyl-P-(1-hydroxy-2-oxopiperidin-3-yl)phosphonamidic acid) (2). A solution of 10% Pd/C (200 mg) in anhydrous THF/MeOH (2:3) was stirred at 25°C. A balloon of H_2 was added and the solution vented for 10 minutes. A second balloon of H_2 was then added, and the solution stirred for 1 h. Then, this slurry was transferred to a vial containing BnFLM38 (250 mg, 668 mmol) and was allowed to stir for 1 h. The reaction was filtered and concentrated to a yellow oil. Analysis by ESI+ (Expected $[M+H]^+$=285.25 Observed $[M+H]^+$=285.34).

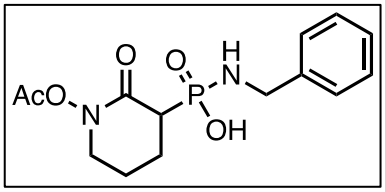

P-(1-acetoxy-2-oxopiperidin-3-yl)-N-benzylphosphonamidic acid (3). To a solution of (**2**) (65 mg, 229 μmol) in anhydrous MeCN (500 uL), Ac_2O (65 μL, 668 μmol) was added. The reaction stirred for 3 h at 25°C. Then, the reaction was concentrated and lyophilized for 2 days. Analysis by ESI+ (Expected $[M+H]^+$=327.29 Observed $[M+H]^+$=327.23). **^{13}C NMR** (75 MHz, $CDCl_3$) δ168.01 (s, 1C), 161.65 (d, J=6.32 Hz, 1C), 141.92 (d, J=6.96 Hz, 1C), 128.22 (s, 2C), 127.55 (s, 2C), 126.54 (s, 1C), 51.63

(s, 1C), 43.24 (s, 1C), 36.42-35.29 (d, J=170.11 Hz, 1C), 25.48 (s, 1C), 25.14 (5.93 Hz, 1C), 22.13 (d, J=7.06 Hz, 1C). **^{31}P NMR** (121 MHz, $CDCl_3$) δ 17.50 (s, 1P).

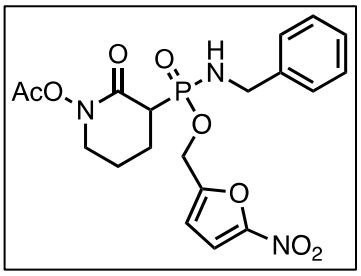

3-((benzylamino)((5-nitrofuran-2-yl)methoxy)phosphoryl)-2-oxopiperidin-1-yl acetate (4). To a solution of (**3)** (73 mg, 224 mmol) in anhydrous acetonitrile, 2-(bromomethyl)-5-nitrofuran (138.26 mg, 671 mmol) were added. The reaction was allowed to stir at 50°C for 20 h. The solvent was then removed and the reaction was purified via reverse-phase HPLC. This was then lyophilized to a yellow solid. Analysis by ESI+ (Expected $[M+H]^+$=452.37. Observed $[M+H]^+$=452). **^{1}H NMR** (300 MHz, $CDCl_3$) 7.26-7.23 (m, 6H), 7.17-7.12 (d, J=3.82 Hz, 1H), 6.49 (d, J=7.12 Hz, 2H), 4.89 (m, 2H), 4.36 (d, J=3.22 Hz, 2H), 4.22 (d, J=5.92 Hz, 2H), 3.62 (m, 2H), 3.04 (dt, J=23.40, 7.58 Hz, 1H), 2.13 (s, 3H), 1.96 (s, 2H), 1.18 (s, 2H). **^{13}C NMR** (75 MHz, $CDCl_3$) δ 170.19 (s, 1C), 167.26 (d, J=15.44 Hz, 1C), 153.35 (d, J=9.55 Hz, 1C), 152.60 (s, 1C), 140.09 (d, J=2.07 Hz, 1C), 128.83-127.24 (m, 5C), 112.62-111.99 (m, 2C), 57.39 (s, 1C), 51.37 (s, 1C), 44.46 (s, 1C), 43.61 (d, J=62.07 Hz, 1C), 22.52 (d, J=6.32 Hz, 1C), 20.67 (d, J=2.58 Hz, 1C), 18.2 (s, 1C). **^{31}P NMR** (121 MHz, $CDCl_3$) δ 29.49 (s, 1P).

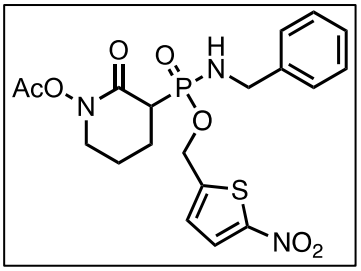

3-((benzylamino)((5-nitrothiophen-2-yl)methoxy)phosphoryl)-2-oxopiperidin-1-yl acetate (5). To a solution of (**3**) (6 mg, 19 mmol) in anhydrous $CHCl_3$, (5-nitrothiophen-2-yl)methanol (4.39 mg, 28 mmol) were added, followed by triphenylphosphine (7.2 mg, 28 mmol). Then, DIAD (5.4 μL, 28 mmol) were added. The reaction was allowed to stir at 25°C for 20 h. The solvent was removed and the crude product was purified via reverse-phase HPLC. This was then lyophilized to an orang e solid. Analysis by ESI+ (Expected $[M+H]^+$=468.43. Observed $[M+H]^+$=468.49). **^{31}P NMR** (121 MHz, $CDCl_3$) δ 29.34 (s, 1P), 29.25 (s, 1P) *isomers*.

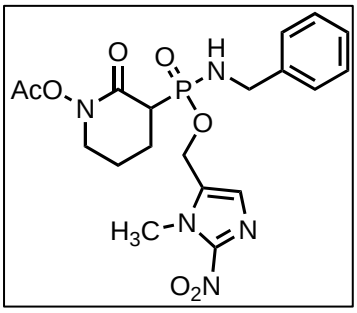

3-((benzylamino)((1-methyl-2-nitro-1H-imidazol-5-yl)methoxy)phosphoryl)-2-oxopiperidin-1-yl acetate (6). To a solution of (**3**) (46 mg, 141 mmol) in anhydrous $CHCl_3$, (1-methyl-2-nitro-1*H*-imidazol-5-yl)methanol (33 mg, 211 mmol) were added, followed by triphenylphosphine (55 mg, 211 mmol). Then, DIAD (42μL, 211 mmol) were added. The reaction was allowed to stir at 25°C for 20 h. The solvent was removed and the crude product was purified via reverse-phase HPLC. This was then lyophilized to a yellow solid. Analysis by ESI+ (Expected $[M+H]^+$=468.43. Observed $[M+H]^+$=468). **^{1}H NMR** (500 MHz, $CDCl_3$) δ 7.46 (s, 1H), 7.32 (m, 5H), 4.85 (d, J=18.92 Hz, 2H), 4.26 (d, J=7.55Hz, 2H), 3.60 (m, 2H), 3.17 (dt, J=13.12Hz, J=87.86Hz, 1H), 2.17 (s, 3H), 2.14 (m, 1H), 2.04-1.92 (m, 2H), 1.63 (m, 1H). **^{13}C NMR** (125 MHz, $CDCl_3$) δ 170.14 (s, 1C), 167.03 (s, 1C), 146.32 (m, 1C), 139.94 (m, 1C), 128.73 (s, 1C), 128.53

(s, 2C), 127.47 (m, 3C), 54.83 (s, 1C), 51.17 (s, 1C), 44.62 (s, 1C), 43.64 (d, J=128.67Hz, 1C), 21.99 (s, 1C), 20.56 (s, 1C), 18.01 (s, 1C). **^{31}P NMR** (202.4 MHz, $CDCl_3$) δ 29.53 (s, 1P), 29.23 (s, 1P) *isomers*.

3. Cell culture experiments.

Cell viability assay. Cell viability was determined by crystal violet staining, as previously described[3,4].The cell lines used were D423 (*ENO1*-deleted), D423 ENO1 (overexpressing *ENO1*) and LN319 (control). Glioma cells were seeded in 96-well plates and treated with varying concentrations of the inhibitors described above for 7 days. Cells were then washed with PBS, fixed with 10% formalin and stained with 0.05% crystal violet. Washed and dried plates were dye-extracted using 10% acetic acid, and absorbance was measured at 595 nm using Omegastar Plate Reader (BMG Labtech). To test the efficacy of the synthesized under hypoxic conditions, 1 x 10^4 cells were plated in 96-well plates, treated with inhibitor and incubated for 3 days in a hypoxia station (Don Whitley Scientific, Shipley, UK) set at 1% O_2 and 5% CO_2. Crystal violet staining was then performed as described above.

Representative plates for VCY15, VCY16, VCY17, POMHEX, TH-302

VCY15

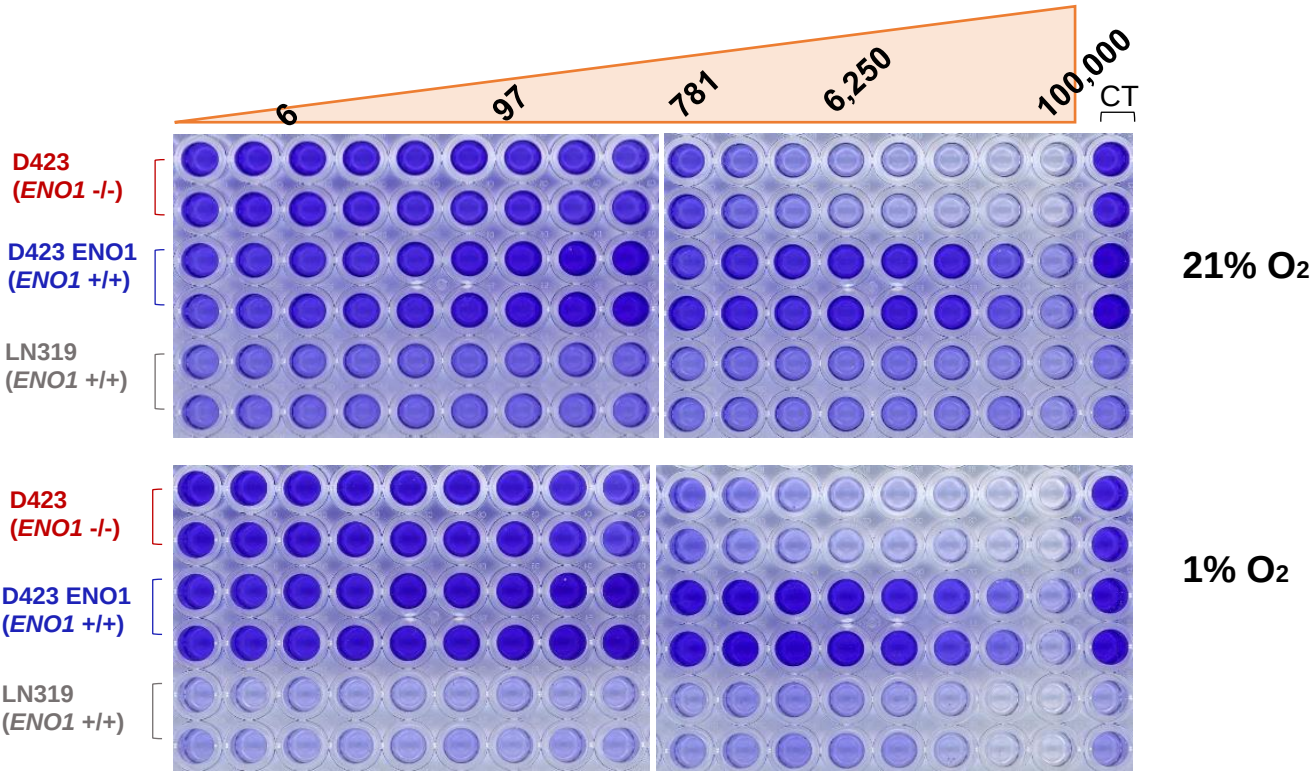

VCY16

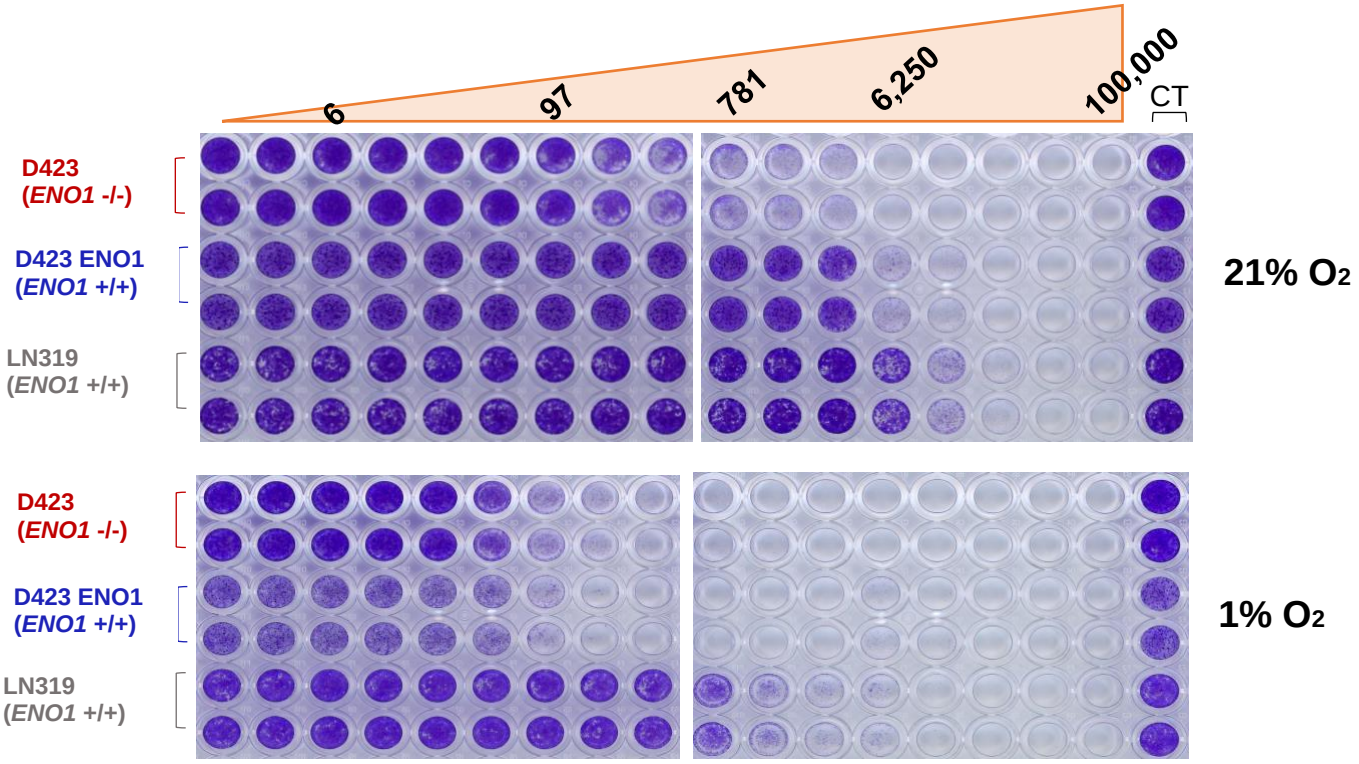
6
97
781
6,250
100,000
CT
D423
(ENO1 -/-)
D423 ENO1
(ENO1 +/+)
LN319
(ENO1 +/+)
21% O2
D423
(ENO1 -/-)
D423 ENO1
(ENO1 +/+)
LN319
(ENO1 +/+)
1% O2

VCY17

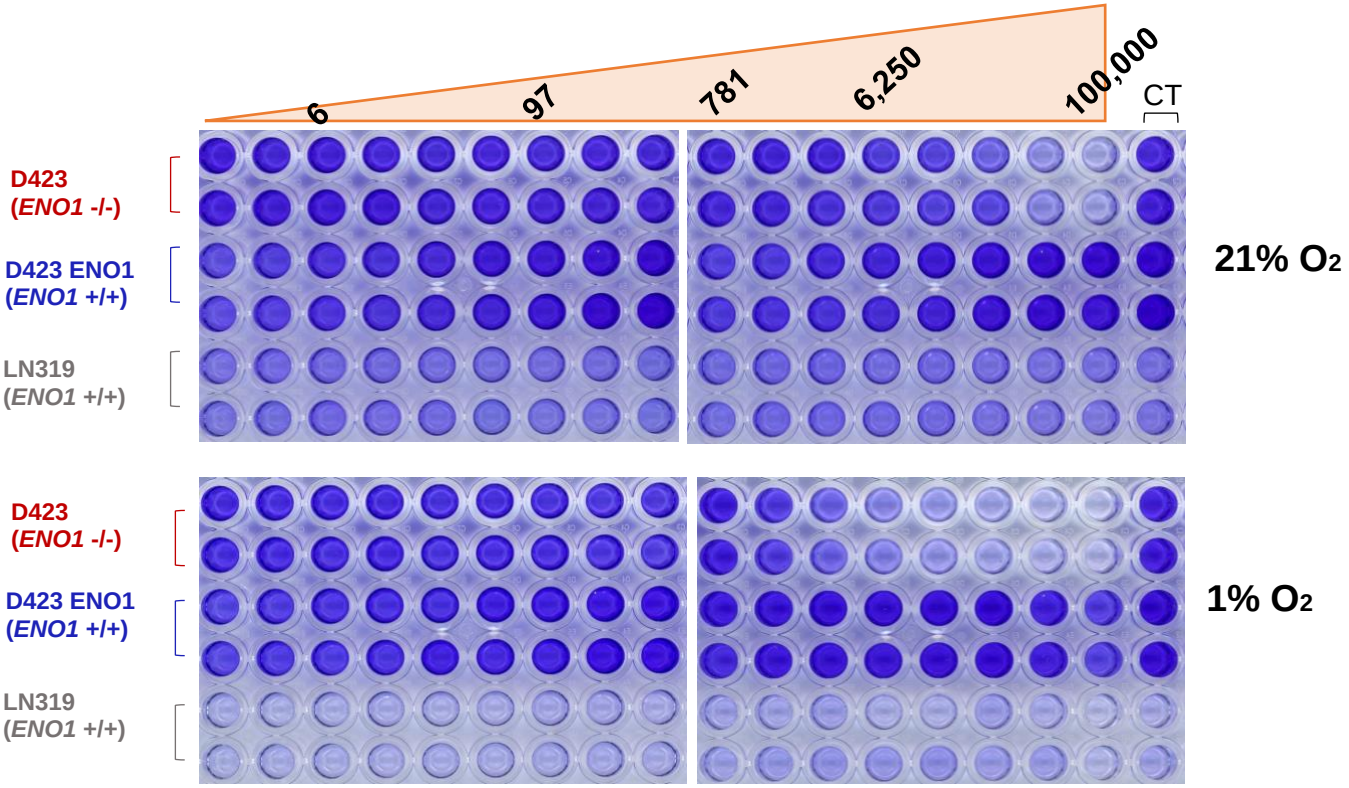
6
97
781
6,250
100,000
CT
D423
(ENO1 -/-)
D423 ENO1
(ENO1 +/+)
LN319
(ENO1 +/+)
21% O2
D423
(ENO1 -/-)
D423 ENO1
(ENO1 +/+)
LN319
(ENO1 +/+)
1% O2

POMHEX

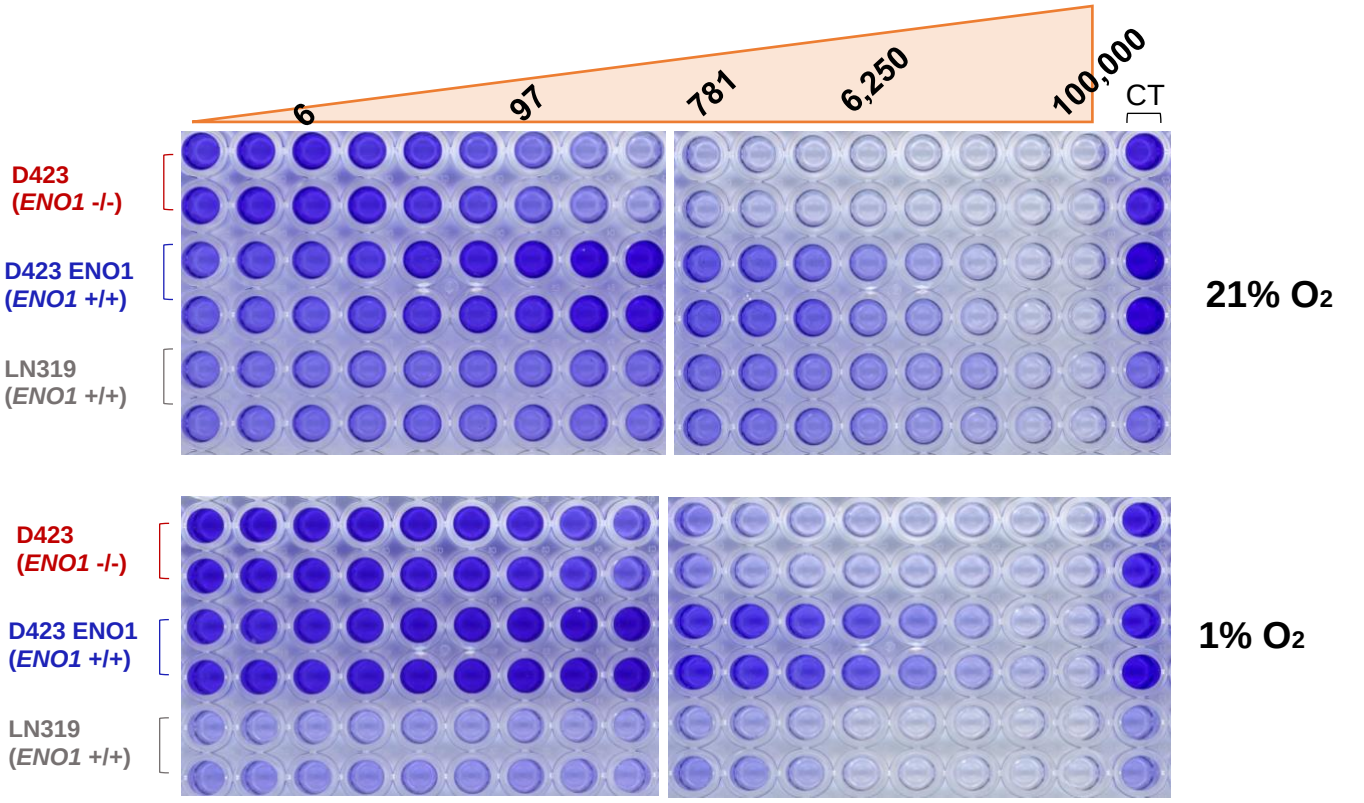

TH-302

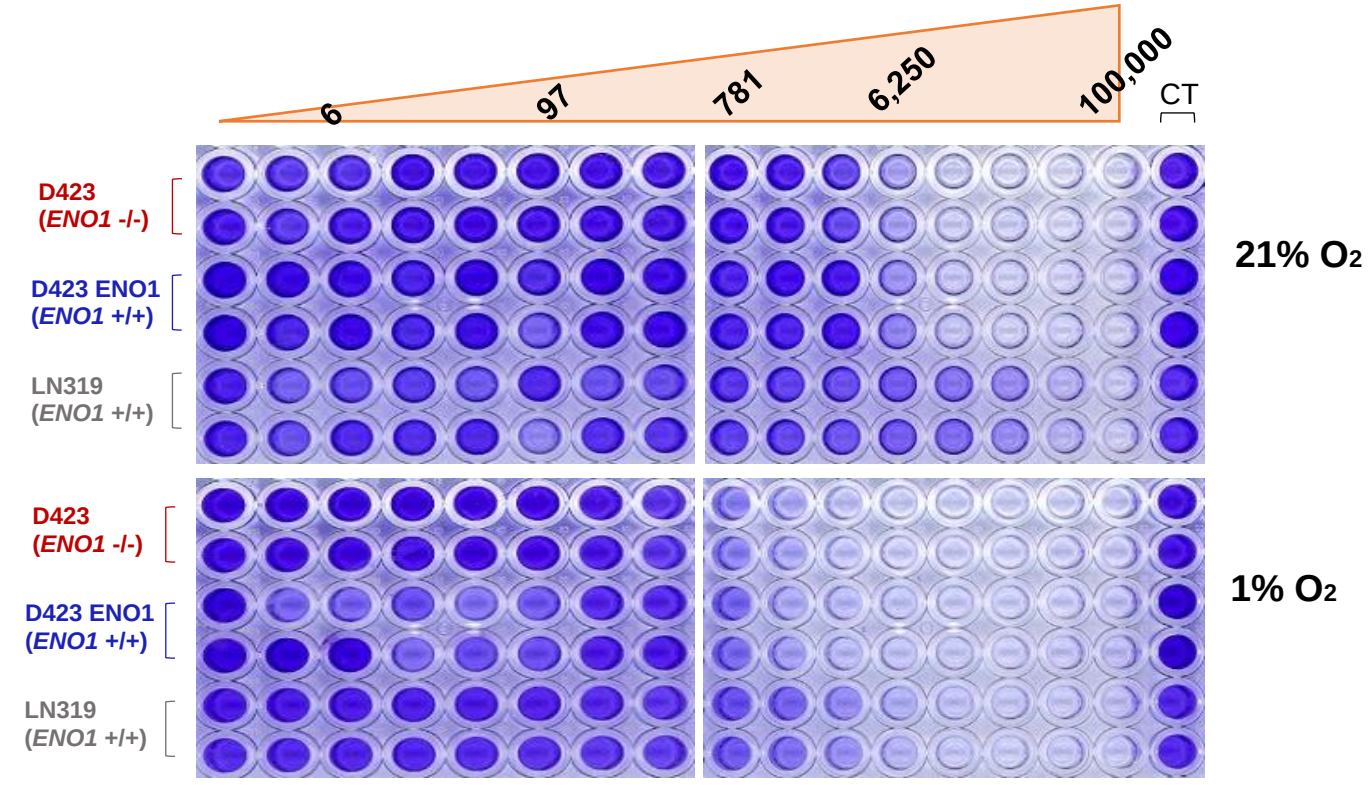

VCY17: 7% O_2

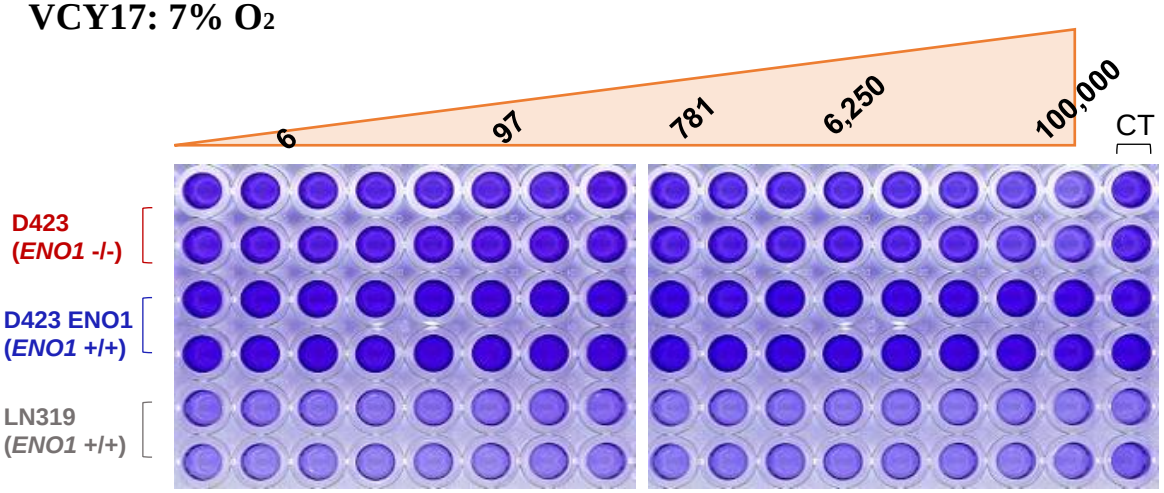

VCY17: 21% O_2

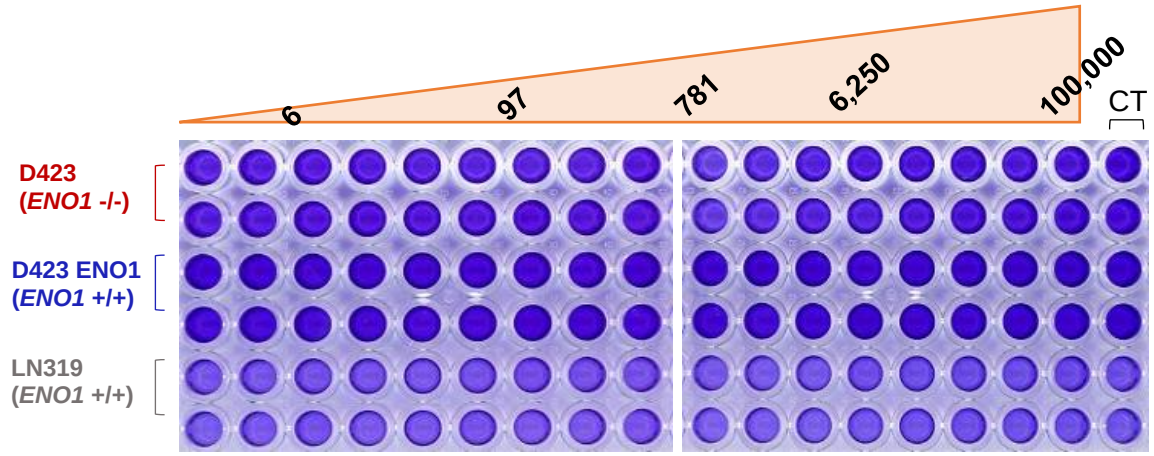

4. References

(1) Lin, Y.-H.; Satani, N.; Hammoudi, N.; Ackroyd, J. J.; Khadka, S.; Yan, V. C.; Georgiou, D. K.; Sun, Y.; Zielinski, R.; Tran, T.; et al. Eradication of ENO1-Deleted Glioblastoma through Collateral Lethality. *bioRxiv* **2018**, 331538.

(2) Muller, F. L.; Colla, S.; Aquilanti, E.; Manzo, V. E.; Genovese, G.; Lee, J.; Eisenson, D.; Narurkar, R.; Deng, P.; Nezi, L.; et al. Passenger Deletions Generate Therapeutic Vulnerabilities in Cancer. *Nature* **2012**, *488*, 337–343.

(3) Leonard, P. G.; Satani, N.; Maxwell, D.; Lin, Y.-H.; Hammoudi, N.; Peng, Z.; Pisaneschi, F.; Link, T. M.; Lee, G. R.; Sun, D.; et al. SF2312 Is a Natural Phosphonate Inhibitor of Enolase. *Nat. Chem. Biol.* **2016**, *12* (12), 1053–1058.

(4) Satani, N.; Lin, Y.-H.; Hammoudi, N.; Raghavan, S.; Georgiou, D. K.; Muller, F. L. ENOblock Does Not Inhibit the Activity of the Glycolytic Enzyme Enolase. *PLoS One* **2016**, *11* (12), e0168739.